

Mass Transfer in WD-WD Binaries

Efrain Perez

This thesis is submitted in partial completion of the requirements of the BS
Astronomy-Physics Major.



Astronomy Department
University of Virginia
Charlottesville, VA. USA
May 14th, 2021

Abstract

White dwarf- white dwarf binaries lose orbital angular momentum from gravitational wave luminosity emission and mass transfer. Once a star in a binary, for example, expands via its red giant branch it begins to overflow its Roche lobe. This overflow can cause the binary to experience unstable mass transfer leading to the merger of the two stars. Stable mass transfer can also occur in which the Roche lobe is filled but not enough to cause unstable transfer. For this paper we will examine mass transfer of newly created white dwarfs using MESA stellar evolution software.

Contents

| | | |
|----------|---|-----------|
| 1 | Introduction | 2 |
| 2 | MESA Simulations | 5 |
| 2.1 | MESA | 5 |
| 2.2 | Pre-Main sequence star to white dwarf model | 5 |
| 2.2.1 | 0.1M \odot Helium Core Star | 6 |
| 2.2.2 | 0.2M \odot Helium core star | 7 |
| 2.2.3 | 0.4M \odot Helium core star | 9 |
| 3 | Mass Transfer in Binaries | 12 |
| 3.0.1 | Roche Lobe | 12 |
| 3.0.2 | Gravitational Wave Radiation | 13 |
| 4 | WD-WD Binary MESA Model | 17 |

Chapter 1

Introduction

A main sequence star is destined to become a white dwarf after its nuclear burning phases have ended. The majority of the star's lifetime will be spent on the main sequence branch converting hydrogen into helium([Icko Iben, 1991]). After this burning is finished, the star rapidly evolves onto the giant branch in which it burns hydrogen in a thin shell outside the core. The core at this stage is contracting and heating, and is mostly made of helium.

Once the star's central temperature reaches around 10^8K and the central density reaches 10^4 g cm^3 it begins to ignite helium in the center. After helium ignition at the tip of the giant branch, the star moves to the horizontal branch. This marks the beginning of the helium burning in a steadily growing convective core. The hydrogen shell burning is still the main contributor to the star's surface luminosity, so the mass of the hydrogen exhausted core grows despite the convective core within it converting helium into carbon and oxygen[Icko Iben, 1991]. The abundance of helium in the center eventually declines, the helium exhausted core contracts and heats up. This occurs while the hydrogen rich envelope begins to expand and cool.

As the star is continuing to evolve, it enters a new stage in which the convective envelope extends inward, crosses the hydrogen helium interface and begins to enter into layers in which hydrogen has been depleted. This hydrogen has been fully converted into helium while most of the original carbon and oxygen has been converted to nitrogen. The base of the convective envelope begins to move inward in mass while the helium burning shell moves outward in mass. As they approach each other, the base of the convective envelope heats up, becoming

more dense as it approaches the helium shell. This lead to hydrogen being reignited, which forced the base of the convective envelope to retreat outward in mass in front of the newly formed hydrogen shell[Icko Iben, 1991].

Hydrogen re-ignition leads to compression in the helium exhausted core. The matter within this core becomes so compressed that the electrons become degenerate. Electron conduction thereafter helps maintain core temperature within a factor of 2 of the mean core temperature. Due to the high densities and core temperature, neutrino losses via plasma and photo-neutrino processes become important while much of the outer mass is expelled due to this stellar wind. Alas we are left with a white dwarf.

The main mechanism responsible for mass transfer in this paper, is Roche lobe overflow. Roche lobe is an area around a star in which matter is gravitational bound to it. In short, consider a point test particle in a gravitational potential produced by two masses orbiting each other, each producing their own gravitational force. In our case, one assumes the test particle does not contribute ant gravitational attraction due to the two masses being very massive in comparison. One also assumes the two masses(stars) follow circular, keplerian orbits. There is one unique point in this equipotential that has two separate parts(lobes). These two lobes touch at a single point along a line joining the two centers of the compact binary[Jolien D. E. Creighton and Creighton, 2011]. Each of these lobes is referred to a Roche lobe.

Common envelope formation is another mechanism by which a binary system may loss mass and angular momentum, and through which the orbit may shrink drastically. A common envelope occurs when both the Roche lobes are filled, more matter from the primary donor star spills into both lobes creating this "common envelope." Friction is generated between the matter within this common envelope and the stellar cores. This in turn creates a torque on the stellar cores forcing them closer together.

Gravitational wave(GW) emission of energy and angular momentum from the binary systems is another mechanism by which it loses orbital angular momentum. The separation needed for GW inspiral to occur in a Hubble time is $1.5 - 3R_{\odot}$, in short the binary possesses a mass quadruple moment and the time for the components to come into contact[Icko Iben, 1991]. It gives a time until coalescence of around $10^8 - 10^{10}$ years for typical initial separations

after mass transfer has occurred. This time is solely dependent on the initial separation and individual binary masses which we will see later in this paper[Jolien D. E. Creighton and Creighton, 2011].

Chapter 2

MESA Simulations

2.1 MESA

The software used to build stellar models is Modules for Experiments in Stellar Astrophysics (MESA). MESA stellar evolution software was used for all model building in this paper. There were several built in models within MESA that were used along with a custom model built for a specific function.

2.2 Pre-Main sequence star to white dwarf model

This model goes through three different branches in its evolutionary track, ending at a white dwarf. The starting point was a pre-main sequence model with initial composition $X = 0.72$, $Y = 0.27$ and $Z = .01$. It was then evolved until the center of the star had burned hydrogen to helium, creating helium core masses of size 0.1 , 0.2 and $0.4M_{\odot}$, respectively. The first branch is responsible for evolving the pre-main sequence star through the main sequence branch, up the red giant branch and leading into becoming a white dwarf. The second branch is a part of MESA's "stellar engineering" in that it takes layers off the star until it becomes a white dwarf and begins its cooling track. The third branch is the white dwarf cooling track of the pre-main sequence star.

2.2.1 $0.1M_{\odot}$ Helium Core Star

Figure 2.1 and 2.2 shows the HR diagrams for the three separate branches for a $0.1M_{\odot}$ helium core. The time scale ranges from $0 - 10^9$ years showing the main sequence branch, red giant branch, white dwarf and white dwarf cooling track.

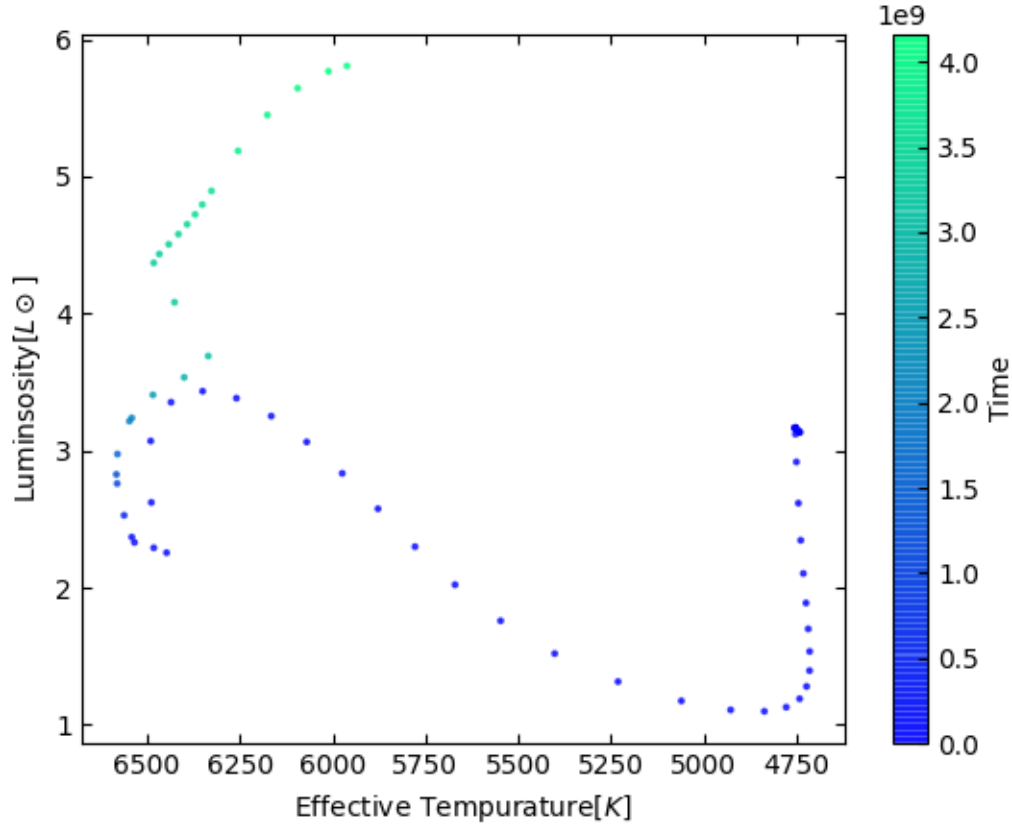


Figure 2.1: HR diagram of pre-main sequence, main sequence and giant branch of a $0.1M_{\odot}$ helium core star.

Figure 2.1 above displays an HR diagram of the various branches mentioned. It is worth noting that the x-axis is inverted to show higher values on the left and vice versa. It is also color coded to show where the star spends the most time. The star spends most of its time upwards in the $4-6L_{\odot}$ range which also corresponds to high temperatures. This plot shows pre-main sequence branch, main sequence and red giant branch. The pre-main sequence branch is the shortest and occurs towards the right side at about $4750K$ before starting the

main sequence branch that ranges from 4750-6500K.

Figure 2.2 shows the newly formed white dwarf and its sequential cooling track. This is after the star has experienced its envelope loss through stellar winds and becoming a planetary nebulae. The star is at its hottest after being stripped of its layers leaving a bare helium core. Figure 2.2 then shows the remaining cooling track of this white dwarf in a red color scheme. In a span of 10^8 years, the white dwarf reaches below $.001L_{\odot}$.

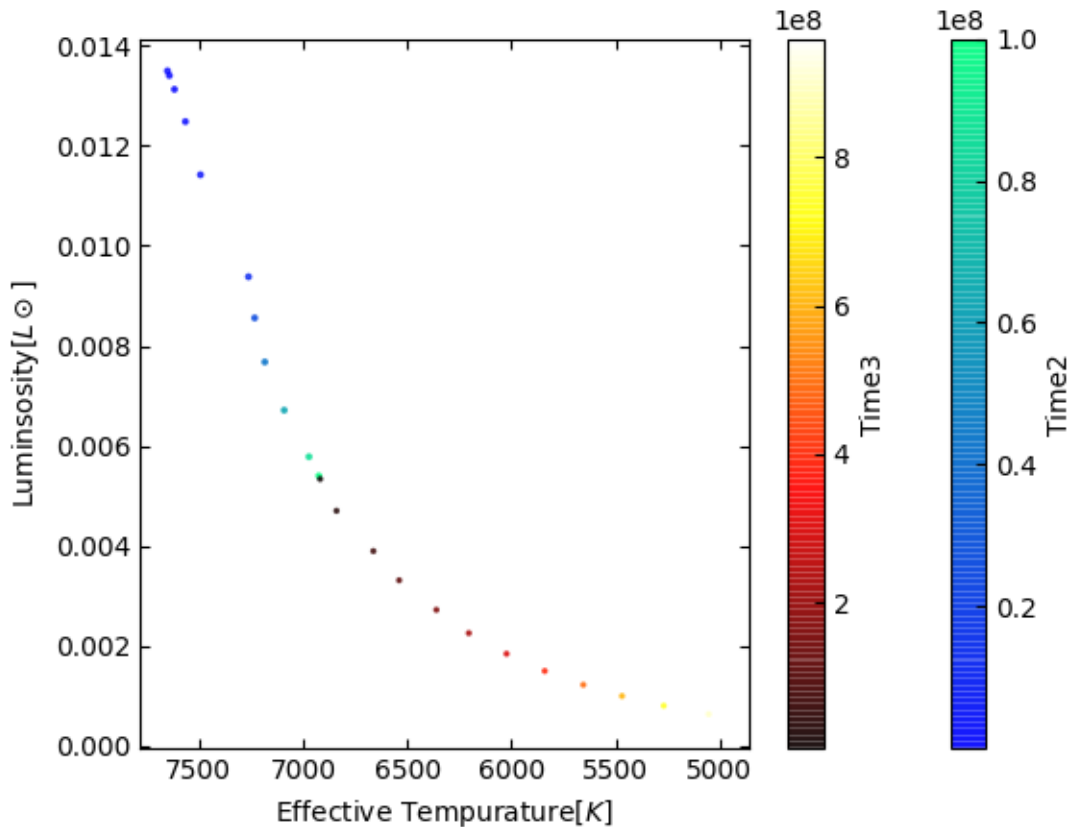


Figure 2.2: HR diagram shows the combined sequence of the newly formed white dwarf and its associated cooling sequence

2.2.2 $0.2M_{\odot}$ Helium core star

Figure 2.3 shows the same branches as the previous star mentioned above. There are several differences, to start the luminosity range is much higher. Once hydrogen has depleted in the

core, the amount of helium collapsing and heating up is much higher. This causes the outer hydrogen shell around the core to heat up more which forced star to get brighter and redder which is why it actually cools.

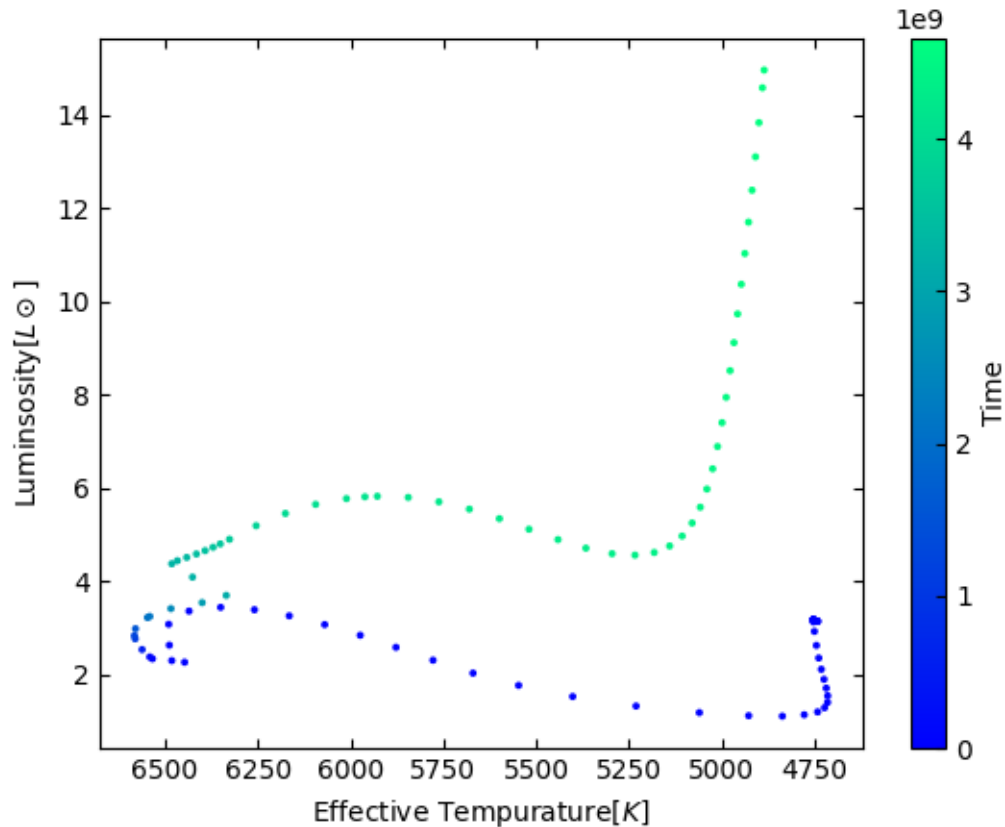


Figure 2.3: HR diagram shows the pre-main, main and red giant branch of the $0.2M_{\odot}$ helium core star.

Figure 2.4 shows the start of the formation of the white dwarf. This white dwarf is starting to cool after losing its envelope from a strong stellar wind. The majority of the white dwarfs time is spent actually towards the end of its sequence during its cooling track. The white dwarf starts cooling at super high temperature. This increase in temperature is due to the formation a nebula that shines due to the strong irradiation by the hot star.

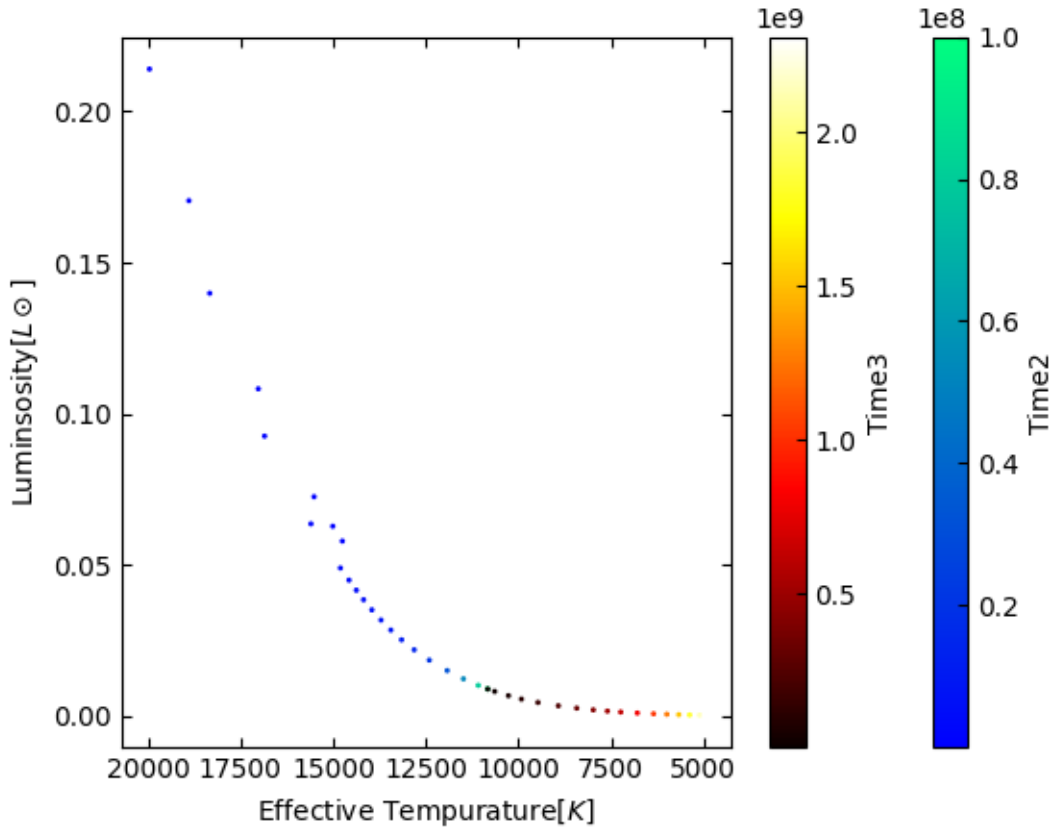


Figure 2.4: HR diagram shows the combined sequence of the newly formed white dwarf and its associated cooling sequence

2.2.3 $0.4M_{\odot}$ Helium core star

Figure 2.5 shows the pre-main sequence, main sequence and red giant branch. This star leaves the first branch with the highest luminosity peaking at about $10^3 L_{\odot}$.

Once the star passes has lost its layers it begins its white dwarf sequence at 60000K, making it the hottest white dwarf of the group. Figure 2.6 displays the cooling sequence of the white dwarf. Not only does the white dwarf drop in luminosity but also in effective temperature. The stage in the star's life right after its layers have been ripped off leaving a bare helium core will be used as our stars in our binary simulation. In the next section I will explain the binary evolution model.

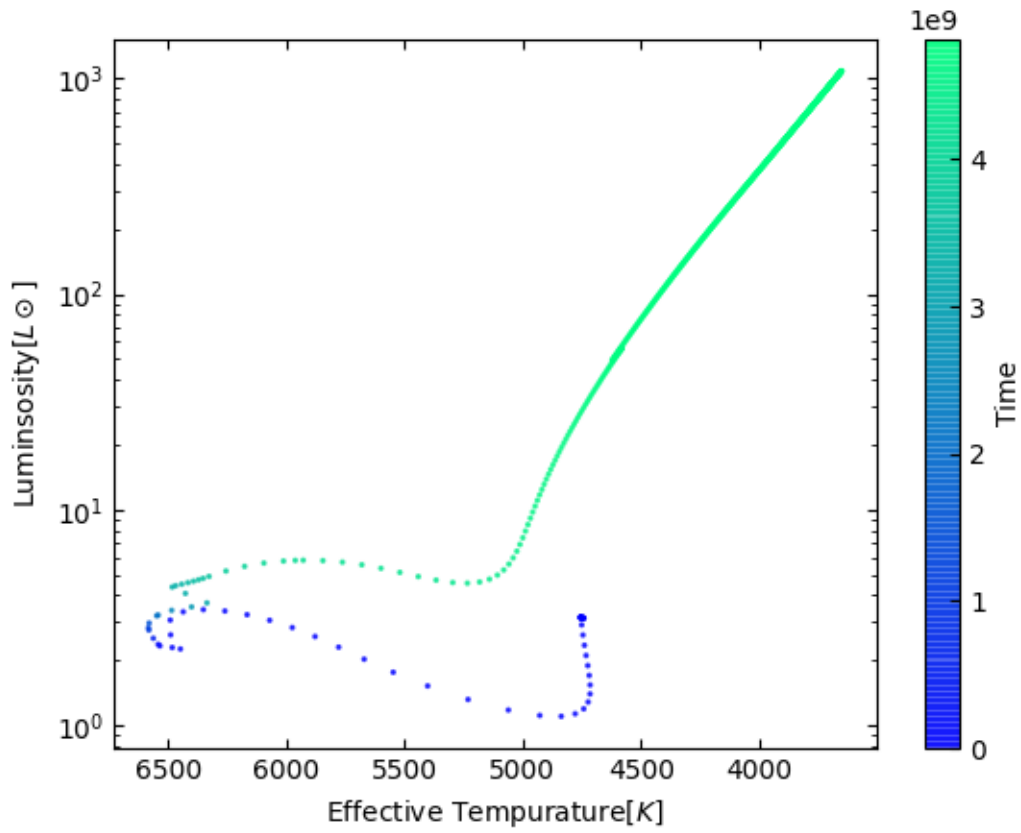


Figure 2.5: HR diagram shows the combined sequence of the newly formed white dwarf and its associated cooling sequence

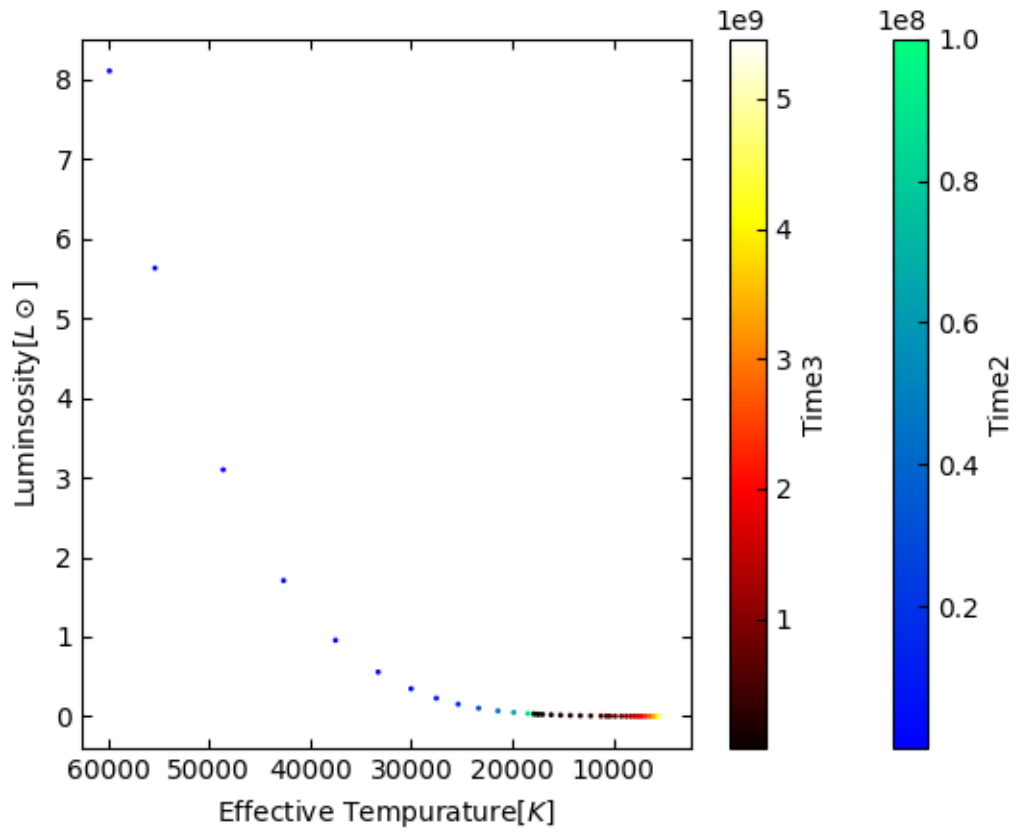


Figure 2.6: HR diagram shows the combined sequence of the newly formed white dwarf and its associated cooling sequence for a $0.4M_{\odot}$ helium core star.

Chapter 3

Mass Transfer in Binaries

3.0.1 Roche Lobe

Continuing our discussion of Roche Lobes from the introduction section, considering a point particle being influenced by the gravitational potential of the two masses orbiting each other. This particle does not contribute any gravitational attraction and the two masses follow circular, keplerian orbits. The two lobes intersect at a single point along a line connecting the two centers of the binary(ref icko iben jr). A common quantity used to describe a binary system is q , where $q = \frac{M_2}{M_1}$ is the ratio of the two masses in the binary. Since there is gas flowing, this dynamic is governed by Euler's equation which is corrected for this rotating frame and the centrifugal and Coriolis force s.

$$\frac{\partial \mathbf{v}}{\partial t} + (\mathbf{v} \cdot \nabla) \mathbf{v} = -\nabla \Phi_R - 2\boldsymbol{\omega} \times \mathbf{v} - \frac{1}{\rho} \nabla P \quad (3.1)$$

The angular velocity is represented by $\boldsymbol{\omega}$, the term $-2\boldsymbol{\omega} \times \mathbf{v}$ is the Coriolis force per unit mass, $-\nabla \Phi_R$ is the gravitational and centrifugal force in one term. Finally Φ is the Roche potential and its potential is given by,

$$\Phi_R(\mathbf{r}) = \frac{-GM_1}{|\mathbf{r} - \mathbf{r}_1|} - \frac{GM_2}{|\mathbf{r} - \mathbf{r}_2|} - \frac{1}{2}(\boldsymbol{\omega} \wedge \mathbf{r})^2. \quad (3.2)$$

Plotting this 3D equipotential shows two deep points and a saddle point. Taking a slice of this potential also shows Roche lobe limits and point of transfer. Figure 3.1[Juhan Frank, 2002] shows a slice of (3.2) for $q = 0.25$. The most important lines are the bold black lines

showing the Roche lobes for both stars and the L_1 point, known as the first Lagrange point. This point serves as a passage for matter to transfer between the two stars. For example, if a star starts to approach its Roche lobe limit via stellar evolution it will reach its limit and start to overflow its Roche lobe.

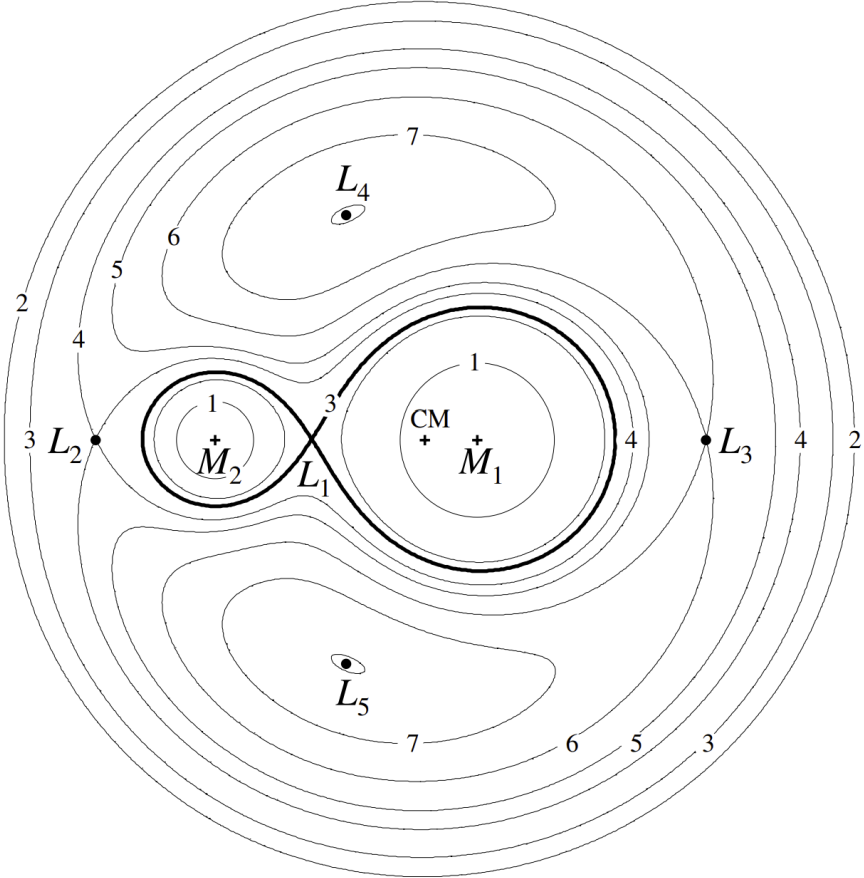


Figure 3.1: Displays a slice of the equipotential from equation 3.2

3.0.2 Gravitational Wave Radiation

As mentioned on the intro, gravitational wave radiation is another mechanism in which the binary loses angular momentum. Consider two particles of mass 1 and mass 2 lying on the x-y plane, so that the angular momentum vector points in the z direction. We can then define the separation, $a = r_1 + r_2$, the total mass $M = m_1 + m_2$ and the reduced mass ,

$\mu = \frac{m_1 m_2}{M}$. In order to find the equation for gravitational wave luminosity produced by a binary system we first need the non-vanishing quadrupole tensors[Jolien D. E. Creighton and Creighton, 2011].

$$I_{11} = \frac{1}{2}\mu a^2(1 + \cos 2\phi) \quad (3.3)$$

$$I_{22} = \frac{1}{2}\mu a^2(1 - \cos 2\phi) \quad (3.4)$$

$$I_{12} = I_{21} = \frac{1}{2}\mu a^2 \sin 2\phi \quad (3.5)$$

The orbital phase uniformly increases with time and is given by $\phi = \omega t$. We next compute the metric perturbation of the non-vanishing quadrupole tensors by two time derivatives[Jolien D. E. Creighton and Creighton, 2011].

$$\ddot{I}_{11} = -2\mu a^2 \omega \cos 2\phi \quad (3.6)$$

$$\ddot{I}_{22} = 2\mu a^2 \omega \cos 2\phi \quad (3.7)$$

$$\ddot{I}_{12} = \ddot{I}_{21} = -2\mu a^2 \omega \sin 2\phi \quad (3.8)$$

We must take into account an observer a distance r in the direction of the orbital angular momentum, the matrix is in the TT gauge. This TT gauge provides the polarization in this direction.

$$h_{ij}^{TT} = -\frac{4G\mu a^2 \omega^2}{c^4 r} \begin{vmatrix} \cos 2\phi & \sin 2\phi & 0 \\ \sin 2\phi & -\cos 2\phi & 0 \\ 0 & 0 & 0 \end{vmatrix} \quad (3.9)$$

Now we can read off the polarization's we were looking for.

$$h_+ = -\frac{4G\mu a^2 \omega^2}{c^4 r} \cos 2\phi \quad (3.10)$$

$$h_x = -\frac{4G\mu a^2 \omega^2}{c^4 r} \sin 2\phi \quad (3.11)$$

The orbital frequency for gravitational waves is observed at twice the orbital frequency, $f = 2f_{orbital} = \frac{\omega}{\pi}$. The loss of energy of the system will cause the orbit to decay, frequency to increase and the radiation amplitude to also increase. The third time derivative of the

quadrupole tensor is needed in order to describe these changes [Jolien D. E. Creighton and Creighton, 2011].

$$I''''_{11} = I''''_{22} = 4 \frac{G}{c^5} \frac{\mu}{M} \left(\frac{v}{c}\right)^5 \sin 2\phi \quad (3.12)$$

$$I''''_{12} = I''''_{21} = 4 \frac{G}{c^5} \frac{\mu}{M} \left(\frac{v}{c}\right)^5 \cos 2\phi \quad (3.13)$$

The matrix is trace free so the gravitational wave luminosity turns out to be,

$$L_{GW} = \frac{1}{5} \frac{G}{c^5} \langle I''''_{11} + I''''_{22} + 2I''''_{12} \rangle = \frac{32}{5} \frac{c^5}{G} \eta^2 \left(\frac{v}{c}\right)^2 \quad (3.14)$$

, where $\eta = \frac{\mu}{M}$. The energy lost come from the Newtonian orbital energy, $E = -\frac{1}{2}\mu v^2$, so $L_{GW} = -\frac{dE}{dt}$, this results in the time until coalescence equation due to gravitational luminosity.

$$\int_{v_0/c}^{\infty} \frac{d\left(\frac{v}{c}\right)^9}{\frac{v}{c}} = \frac{32\eta}{5} \frac{c^3}{GM} \int_0^{\tau_0} dt \quad (3.15)$$

In the above equation, the time until coalescence is given by τ_0 , integrating the equation we are left with,

$$\tau_0 = \frac{5}{256\eta} \frac{GM}{c^3} \left(\frac{c^2 a_0}{GM}\right)^4. \quad (3.16)$$

This equation (3.16) is given in terms of a_0 and M , meaning we can figure out the time until coalescence based on initial separation and masses [Jolien D. E. Creighton and Creighton, 2011].

Figure 3.2 shows the analytic equation of 3.16 plotted for various masses. The largest time being the combination of a $.4M_{\odot}$ and $1M_{\odot}$ star. These are all plotted with the same initial separation of $1R_{\odot}$.

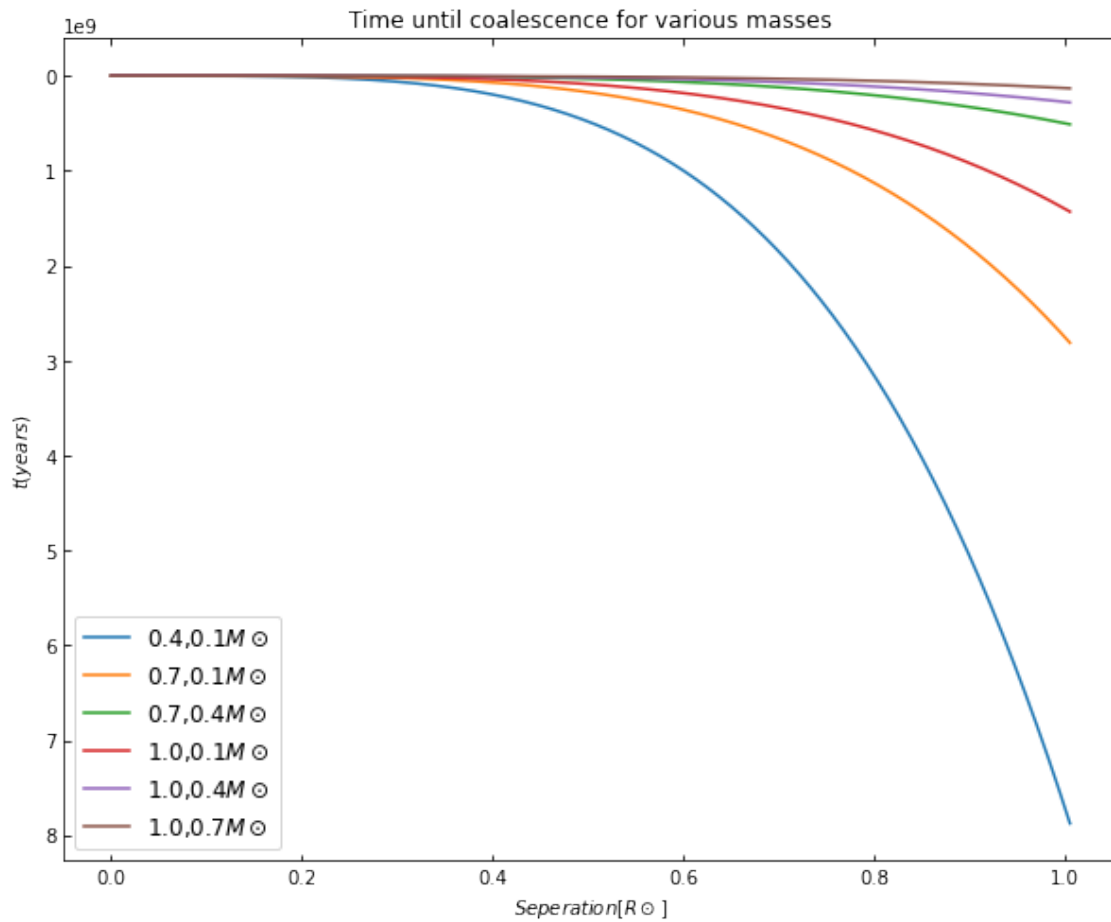


Figure 3.2: Displays the time until coalescence for various mass combinations.

Chapter 4

WD-WD Binary MESA Model

Utilizing MESA's binary evolution test suite, $0.2M_{\odot}$ and $0.1M_{\odot}$ bare helium, newly created white dwarfs were loaded into this model to be evolved. The 0.2 and 0.1 pair is an example of unstable mass transfer. Firstly we will see how the analytical solution of equation (3.16) compares to our simulation. Figure 4.1 shows (3.16) plotted for the initial separation of $.607R_{\odot}$ and the previously mentioned masses. Comparing this to figure 4.2 shows the similarities, the difference the model has not quite reached merge yet which accounts for the slight time difference. This comparison shows that the main mechanism of orbital angular momentum loss leading to mass transfer is GW radiation.

Figure 4.3 shows the systems mass transfer rate M_{\odot}/yr against time. This rate is the absolute value of mass transfer from the donar star that is solely due to Roche lobe overflow(RLOF). The model is also losing angular momentum in addition to GW radiation. Figure 4.4 shows each WDs change in mass against time. There are two points in which there are drastic changes in the binaries mass. It is worth noting that this change also coincides with the spike in mass transfer from figure 4.3.

This WD-WD binary is important in showing the effects of angular momentum loss. In particular the effects of GW radiation and Roche lobe overflow. The model evolves the binary and begins unstable mass transfer due to Roche lobe overfilling. Once unstable mass transfer begins MESA stops the simulation which would need to be modified in order to see the dynamics of a merge.

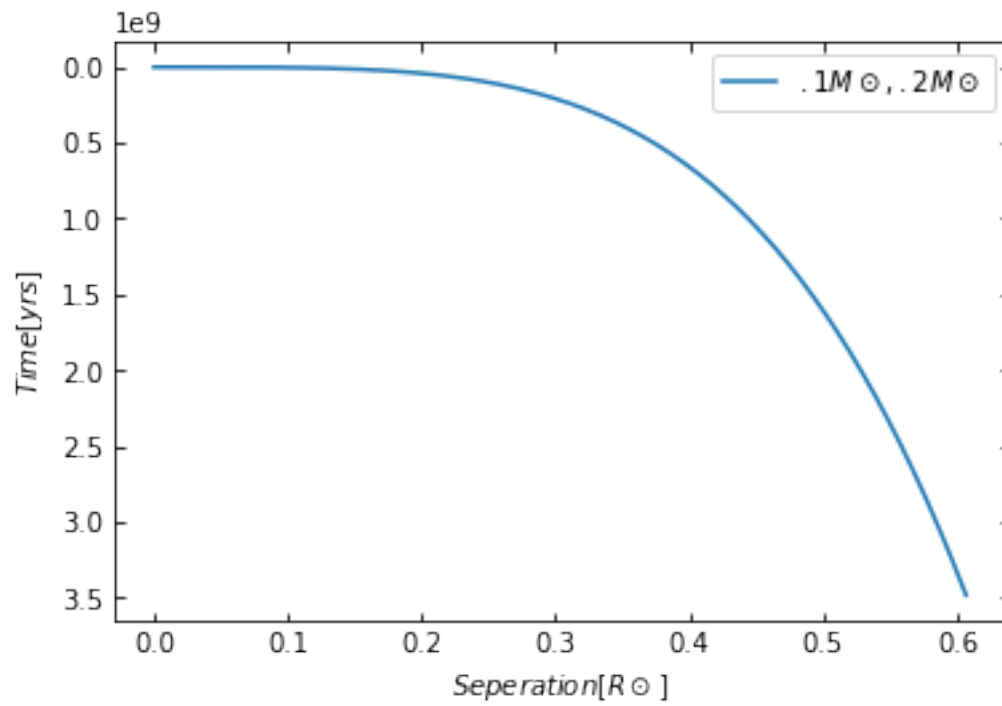


Figure 4.1: The plot shows the time until merge for a 0.2 and 0.1M_⊙ based on the analytic solution of equation (3.16).

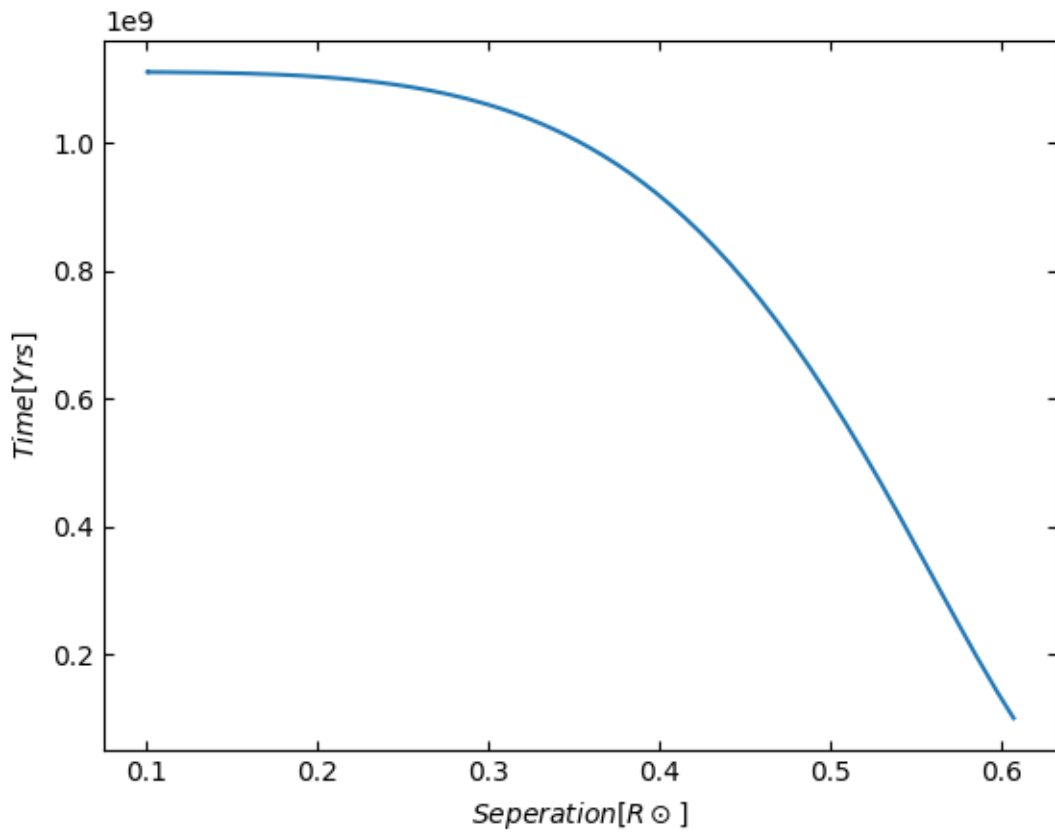


Figure 4.2: The plot shows the time until merge based on the simulated binary of a 0.2 and 0.1 M_{\odot} WDs.

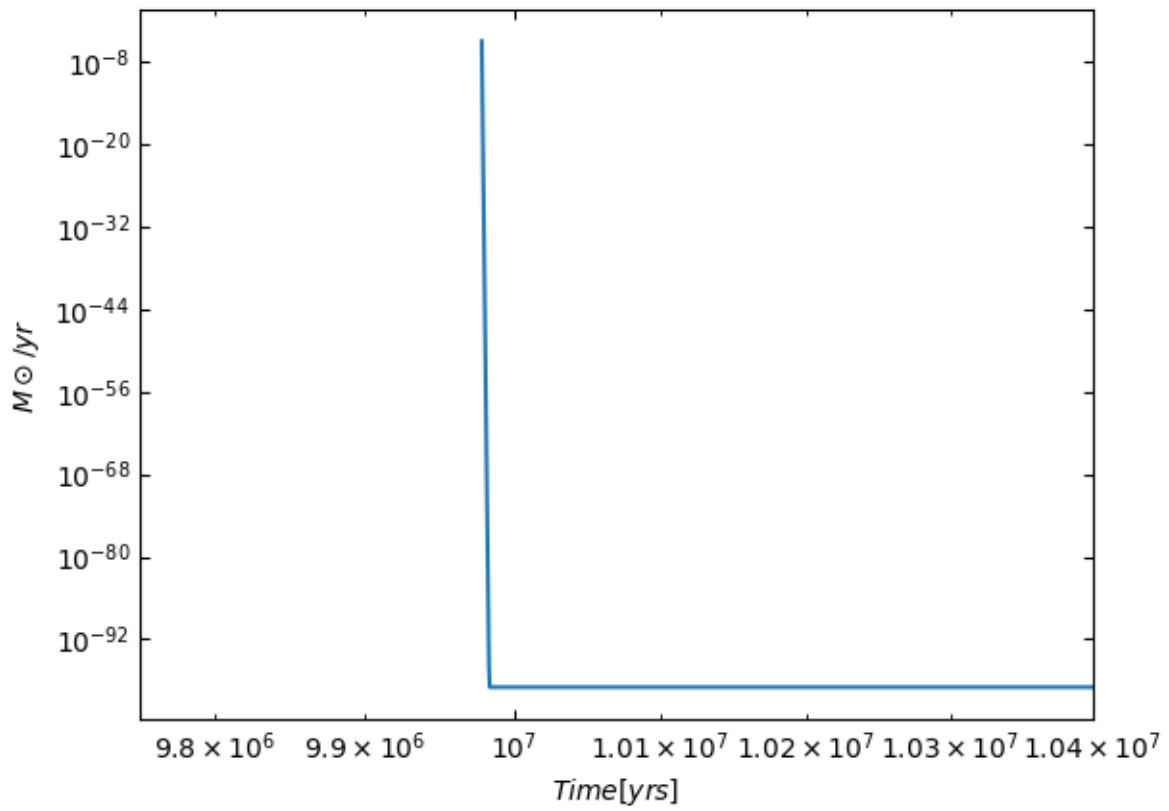


Figure 4.3: Displays the absolute value of mass transfer from the donar star due to RLOF.

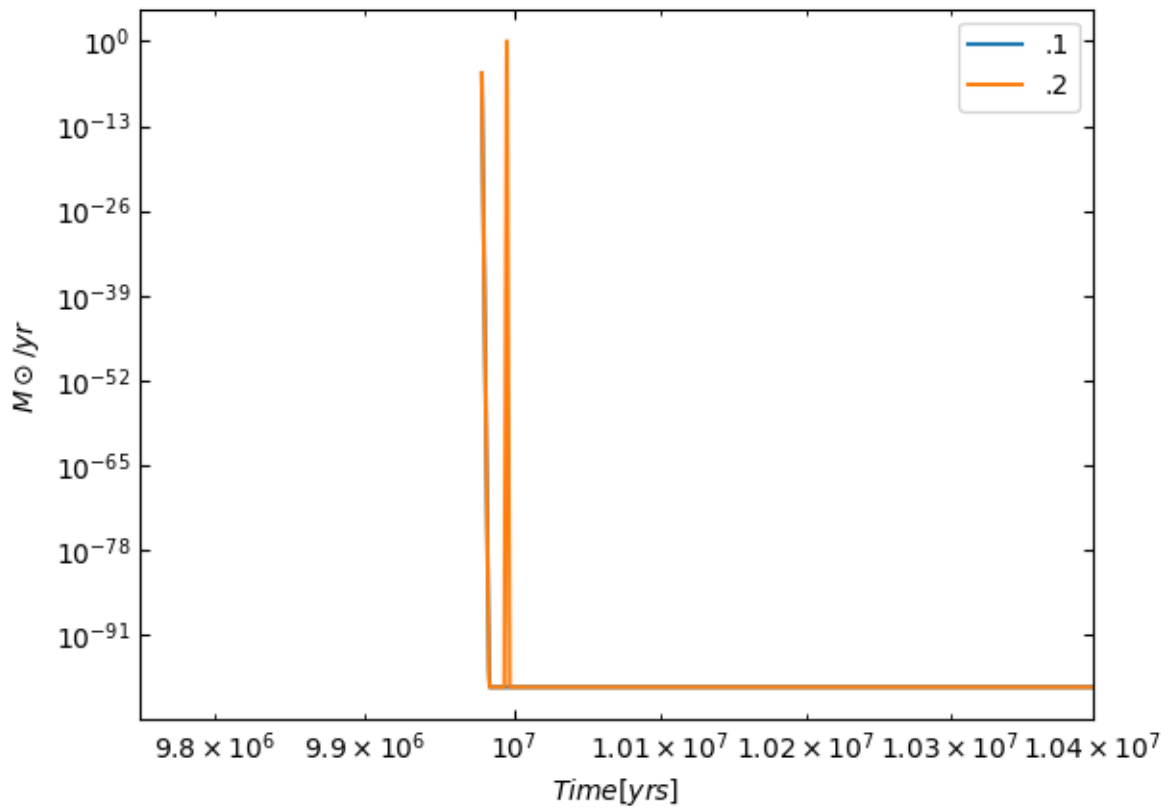


Figure 4.4: The plot shows the change in masses for both WDs in the binary model.

Bibliography

Jr. Icko Iben. Single and binary star evolution. *The Astrophysical Journal*, 1991.

Warren G. Anderson Jolien D. E. Creighton and Jolien Creighton. *Gravitational-Wave Physics and Astronomy : An Introduction to Theory, Experiment and Data Analysis*. John Wiley & Sons, Incorporated, 2011.

Derek Raine Juhan Frank, Andrew King. *Accretion Power in Astrophysics*. Cambridge University Press, 2002.